Anharmonic resonances in the CH chromophore overtone spectra of CHBrF2

Andrea Pietropolli Charmet, Nicola Tasinato, Paolo Stoppa, Santi Giorgianni, Alberto Gambi

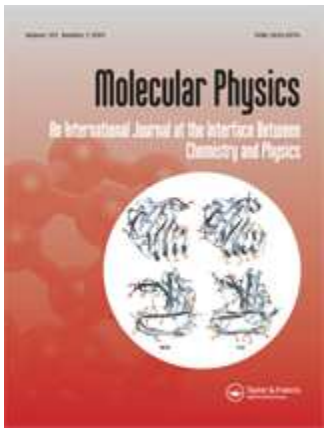

Anharmonic resonances in the CH chromophore overtone spectra of CHBrF2

Journal:	*Molecular Physics*
Manuscript ID:	TMPH-2011-0134.R1
Manuscript Type:	Special Issue Paper - Dijon HRMS
Date Submitted by the Author:	12-Jul-2011
Complete List of Authors:	PIETROPOLLI CHARMET, Andrea; Universita' Ca' Foscari Venezia, Dipartimento di Scienze Molecolari e Nanosistemi TASINATO, Nicola; Universita' Ca' Foscari Venezia, Dipartimento di Scienze Molecolari e Nanosistemi STOPPA, Paolo; Universita' Ca' Foscari Venezia, Dipartimento di Scienze Molecolari e Nanosistemi GIORGIANNI, Santi; Universita' Ca' Foscari Venezia, Dipartimento di Scienze Molecolari e Nanosistemi Gambi, Alberto; University of Udine, Dipartimento di Chimica, Fisica e Ambiente
Keywords:	Overtone spectroscopy, CH chromophore, Fermi and Darling-Dennison resonances, 3D effective Hamiltonian, Second order vibrational perturbation theory

RESEARCH ARTICLE

Anharmonic resonances in the CH chromophore overtone spectra of $CHBrF_2$

Andrea Pietropolli Charmet[*a], Nicola Tasinato[a], Paolo Stoppa[a], Santi Giorgianni[a] and Alberto Gambi[b]

[a]*Dipartimento di Scienze Molecolari e Nanosistemi, Universita' Ca' Foscari Venezia, D.D. 2137, I-30123 Venezia, Italy;* [b]*Dipartimento di Chimica, Fisica e Ambiente, Università degli Studi di Udine, Via Cotonificio 108, I-33100 Udine, Italy.*

Abstract

The gas phase Fourier transform infrared spectra of bromodifluoromethane, $CHBrF_2$, have been recorded up to 10100 cm^{-1} with a resolution of 0.5 cm^{-1}. All the most relevant absorptions in the overtone region have been ascribed to the CH chromophore. 26 bands involving either the CH-stretching (ν_1) and bending (ν_2, ν_7) modes have been assigned and their relative band strengths have been determined. The vibrational analysis of the corresponding polyads (up to N = 7/2) has been performed by means of an effective Hamiltonian which takes into account anharmonic resonances, thus leading to the determination of Fermi and Darling-Dennison coupling terms. The obtained effective spectroscopic parameters have been able to quantitatively describe both the position and intensity of all the absorption bands, and also to rationalize the effects and the magnitudes of the various resonances in each polyad. The results obtained by this approach have been compared with those computed by using high quality *ab initio* electronic structure calculations employing the second order vibrational perturbation theory (VPT2). An overall satisfactory agreement between the observed and the *ab*

* Corresponding author.
Email: jacpnike@unive.it Phone: +39 041 2348541; Fax: +39 041 2348594
Address: Dipartimento di Scienze Molecolari e Nanosistemi, Universita' Ca' Foscari Venezia, D.D. 2137, I-30123 VENEZIA, Italy

initio computed values has been obtained by properly taking into account in the final calculations the relative magnitude of Fermi and Darling-Dennison resonance effects into each polyad.

Keywords: Overtone spectroscopy; CH chromophore; Fermi and Darling-Dennison resonances; 3D effective Hamiltonian; Second order vibrational perturbation theory.

1. Introduction

The analysis of vibrational overtone spectra provides the spectroscopic ground work towards a detailed understanding of intramolecular vibrational energy redistribution (IVR) [1, 2], vibrationally mediated photodissociation (VMP) [3] and infrared resonance multiple photon (IRMP) excitation in the fields of the infrared laser chemistry [4, 5]. The anharmonic couplings among vibrational states, being considered efficient pathways for allowing the vibrational quantum energy in one vibrational mode to be transferred to other modes, strongly influence the overall intramolecular flow of energy among the vibrational degrees of freedom. In a VMP investigation, different experimental techniques are employed to first obtain a vibrationally excited molecule and then to promote it to excited electronic states. The vibrational excitation may strongly influence the course of the following photolysis and so the analysis of the vibrational overtone spectra is useful as a first step for better determining the role of the anharmonic resonances among different molecular vibrations involved in the VMP mechanism. In an IRMP experiment, the timescale of the IVR is one of the key factor ruling the overall process of the excitation by the intense laser field employed. Within this context, one of the most advanced application involves the selective isotope separation. Revealing and determining the anharmonic couplings influencing the energy exchange among vibrational states is therefore of central importance for exploring the intramolecular dynamics and gaining insights in all the processes above mentioned.

Bromodifluoromethane ($CHBrF_2$, halon 1201) belongs to the class of anthropogenic halons, halogenated compounds which are classified among the major sources of reactive bromine in the atmosphere. In accordance to the Montreal protocol,

the production and use of fully halogenated halons, characterized by long atmospheric lifetimes, is now definitely stopped. Bromodifluoromethane, having one CH bond, can react in the troposphere with hydroxyl radicals thus leading to a shorter atmospheric lifetime [6 – 8]. On this basis bromodifluoromethane has been suggested as an interim replacement of fully halogenated halons. In the field of infrared laser chemistry, $CHBrF_2$ has been proposed [9, 10] as working molecule for practical ^{13}C enrichment by IRMP decomposition. In view of these features, we have recently started a detailed investigation on the infrared spectra of bromodifluoromethane. In a first work [11] we have reported on the vibrational analysis of its infrared gas phase spectra in the 200 – 9500 cm^{-1} region coupled to *ab initio* calculations and to the accurate determination of absorption cross sections. Subsequently, a combined microwave and high-resolution infrared study [12] supported by high-level quantum chemical computations has been carried out leading to accurate values of spectroscopic parameters for both the ground and the $v_4 = 1$ vibrational states.

In the present work, we focus on the absorptions due to the CH chromophore [13] in the overtone spectral region up to 10100 cm^{-1}. The results of the vibrational analysis involving the CH-stretching and bending modes, which appear to dominate the near infrared (NIR) spectrum, have led to the determination of Fermi and Darling-Dennison anharmonic coupling terms (together with spectroscopic parameters such as vibrational frequencies and anharmonicity constants), by means of an effective vibrational Hamiltonian approach. Besides, the CH vibrational states have been also analyzed by using *ab initio* electronic structure calculations. In this work, the harmonic part of the *ab initio* force field previously calculated [11] at the CCSD(T) (the acronym stands for coupled cluster with all single and double substitutions augmented with a

quasi-perturbative account for connected triple excitations) level has been scaled in order to achieve a better agreement with the observed fundamental wavenumbers. From this adjusted force field anharmonicity constants, Fermi and Darling-Dennison coupling terms, which are needed to study the absorption of the CH chromophore in the overtone region, have been calculated by means of second order vibrational perturbation theory (VPT2) [14].

2. Experimental details

The synthesis of $CHBrF_2$ has been carried out as previously described [11]. The gas phase infrared spectra have been measured on a Bruker Vertex 70 FTIR spectrometer employing resolutions of 0.2 and 0.5 cm^{-1}. In the spectral region up to 4000 cm^{-1} a 13.4 cm fixed path-length cell fitted with KBr windows has been used, while at higher wavenumbers a White-type multipass cell, with the effective optical path ranging from 10.5 to 77.5 meters, has been employed. All the spectra have been measured at room temperature, and the pressure measurements have been carried out employing capacitance vacuum gauges. For this molecule we have found [11] no significant differences between the determined band intensities from spectra recorded at a resolution of 0.5 cm^{-1} and those obtained from the spectra taken at a resolution of 0.2 cm^{-1} (thus confirming the observation of Orkin et al. [15]). Therefore in this work the band intensities have been derived by employing the spectra recorded at a resolution of 0.5 cm^{-1}, which have a better signal-to-noise ratio. Relative band strengths within a given polyad have been obtained with an experimental uncertainty, estimated as elsewhere described [16, 17], better than 15%.

3. Computational details

The information needed by VPT2 comprises the quadratic, cubic and semi-diagonal quartic force constants. For $CHBrF_2$ this information was calculated in the work of Ref. 11, in which high quality electronic structure calculations at the coupled cluster level of theory were carried out to compute equilibrium geometry and accurate force constants in the space of dimensionless normal coordinates. Here, the details of the computation will be only summarized.

All the calculations were performed at the CCSD(T) [18, 19] level of electronic correlation. Two basis sets of the correlation consistent family of Dunning and co-workers [20], were considered: these are cc-pVTZ and aug-cc-pVTZ. The latter was employed for the fluorine atoms, in both the geometry optimization and the second-order force constant calculations, in order to improve the overestimated C-F stretching frequency [21]; the former basis set (cc-pVTZ) was employed for the other atoms (H, C, Br). The cubic and semi-diagonal quartic force constants were calculated in the normal coordinate space using a finite difference procedure [22] involving displacements along the normal coordinates.

In the present work the VPT2 analysis of the vibrational states has been carried out starting from the resulting hybrid force field (i.e. HYB-2 of Ref. 11). In a first step, to reduce at most the differences between the calculated and observed fundamental wavenumbers, an empirical correction has been performed [23]. Specifically, the harmonic wavenumbers, ω_i, have been corrected according to:

$$\omega_i = \omega_i^0 + \Delta\nu_i \qquad (1)$$

where ω_i^0 are the *ab initio* calculated values and $\Delta\nu_i$ represents the differences between the observed anharmonic wavenumbers and those obtained from VPT2. Therefore, the *ab initio* cartesian harmonic force field has been transformed into a force field in terms of internal coordinates (F_{ij}^0) and scaled to the ω_i :

$$F_{ij} = F_{ij}^0 \sqrt{s_i s_j} \quad (2)$$

where s_i denotes the scaling factors, and F_{ij} represents the improved force constants. Following this procedure, the only significant discrepancies (i.e. greater than 1 cm^{-1}) are found for ν_2 and ν_7. These bands are indeed described as 100% of $R_6 + R_7$ and 100% of $R_6 - R_7$ (where R_6 and R_7 are the internal coordinates associated with the H-C-F angles), respectively. Since the error in the computed wavenumber of ν_2 has opposite sign with respect to the ν_7 one, any attempt to adjust the first value will introduce a larger error on the second one.

4. The effective Hamiltonian for the analysis of the CH polyads

The observed vibrational spectra have been analysed in the framework of a 3D effective Hamiltonian, as defined by Quack and co-workers (see for example Ref. 24 and references therein), which takes explicitly into account Fermi and Darling-Dennison resonances between the CH-stretching (ν_1, *A*' symmetry) and the two CH-bending modes, ν_2 (*A*' symmetry) and ν_7 (*A*" symmetry), corresponding to the in-plane and out-

of-plane CH bending, respectively; in Figure 1 an approximate representation of these modes is shown. Being the frequency of the CH-stretching mode approximately twice the frequency of the CH-deformations, in the spectral region below 3000 cm^{-1} anharmonic resonances among the ν_1 fundamental and the first overtones of ν_2 and ν_7 can occur. Going to higher wavenumbers, these resonances may involve stretching overtones and stretching/bending combination bands, provided that they belong to the same symmetry species. According to this model, the vibrations involving the CH chromophore normal modes can be grouped into different polyads, each of them can be characterized by the polyad number *N* defined as:

$$N = \mathrm{v}_1 + \frac{1}{2}(\mathrm{v}_2 + \mathrm{v}_7) \tag{3}$$

where v_1, v_2 and v_7 are the vibrational quantum numbers for ν_1, ν_2 and ν_7, respectively. The number *N* acts as a sort of label for grouping vibrational states which, to a first approximation, have almost the same energy. Within each polyad the vibrational Hamiltonian has diagonal matrix elements (zero-order states of the polyad) expressed by the following equation

$$\left\langle \mathrm{v}_1, \mathrm{v}_2, \mathrm{v}_7 \mid H^N \mid \mathrm{v}_1, \mathrm{v}_2, \mathrm{v}_7 \right\rangle = \tilde{\nu}_1' \mathrm{v}_1 + \tilde{\nu}_2' \mathrm{v}_2 + \tilde{\nu}_7' \mathrm{v}_7 + x_{11}' \mathrm{v}_1^2 + x_{22}' \mathrm{v}_2^2 + x_{77}' \mathrm{v}_7^2 + x_{12}' \mathrm{v}_1 \mathrm{v}_2 + \\ + x_{17}' \mathrm{v}_1 \mathrm{v}_7 + x_{27}' \mathrm{v}_2 \mathrm{v}_7 \tag{4}$$

where v_1, v_2, v_7 are the above mentioned vibrational quantum numbers, and $\tilde{\nu}_i'$ and x_{ij}' are vibrational wavenumbers and anharmonicities, respectively, treated as adjustable

spectroscopic parameters (values in cm^{-1}) which are refined by the fitting of experimental data. This vibrational Hamiltonian, whose off-diagonal terms couple vibrational states belonging to the same polyad, is block diagonal in N and it has $(N+1)^2$ zero-order states for N integer and $(N + 1/2)(N + 3/2)$ for half integer N. For a molecule belonging to the C_s symmetry point group, each of these blocks, labelled by its own N number, can be further decomposed in two blocks, corresponding to vibrational states having A' or A'' symmetry. Within each block the off-diagonal matrix elements describe the anharmonic resonances. The matrix elements corresponding to the Fermi resonance in which one quantum of CH-stretching is exchanged for two quanta of CH-bending are given by:

$$\left\langle \mathrm{v}_1, \mathrm{v}_2, \mathrm{v}_7 \left| H_F^N \right| \mathrm{v}_1 - 1, \mathrm{v}_2 + 2, \mathrm{v}_7 \right\rangle = \frac{1}{2} k'_{122} \left[\frac{1}{2} \mathrm{v}_1 (\mathrm{v}_2 + 1)(\mathrm{v}_2 + 2) \right]^{1/2} \quad (5)$$

$$\left\langle \mathrm{v}_1, \mathrm{v}_2, \mathrm{v}_7 \left| H_F^N \right| \mathrm{v}_1 - 1, \mathrm{v}_2, \mathrm{v}_7 + 2 \right\rangle = \frac{1}{2} k'_{177} \left[\frac{1}{2} \mathrm{v}_1 (\mathrm{v}_7 + 1)(\mathrm{v}_7 + 2) \right]^{1/2}. \quad (6)$$

Darling-Dennison resonances are taken explicitly into account by the inclusion of the following off-diagonal matrix element:

$$\left\langle \mathrm{v}_1, \mathrm{v}_2, \mathrm{v}_7 \left| H_{D-D}^N \right| \mathrm{v}_1, \mathrm{v}_2 - 2, \mathrm{v}_7 + 2 \right\rangle = \frac{1}{2} k'_{2277} \left[\mathrm{v}_2 (\mathrm{v}_2 - 1)(\mathrm{v}_7 + 1)(\mathrm{v}_7 + 2) \right]^{1/2}. \quad (7)$$

In equations 5 – 7 k'_{ijj} and k'_{iijj} refer to effective spectroscopic resonance parameters. Within each block, the resulting $\mathbf{H}^N$ matrix is diagonalized:

$$\mathbf{Z}_N^{-1}\mathbf{H}^N\mathbf{Z}_N = \mathrm{diag}(E_1^N, E_2^N, ...) \tag{8}$$

thus giving the corresponding eigenvalues E_j^N, which can be compared to the wavenumbers of observed band centres, and the corresponding eigenvector matrix $\mathbf{Z}_N$. The eigenstates are labelled by N_j, where by convention the index j equals to 1 for the highest eigenvalue and it increases with decreasing energy.

Within each polyad the experimental band strength for a given subband is computed according to the following equation:

$$G_j^N = \frac{1}{2.303 \cdot c \cdot l \cdot \tilde{\nu}_0} \int_{\tilde{\nu}_1}^{\tilde{\nu}_2} \log_{10}\left(\frac{I_0}{I}\right) d\tilde{\nu} \tag{9}$$

with c being the concentration (obtained from the pressure of the sample assuming the validity of the ideal gas law), l is the optical path length, $\tilde{\nu}_0$ is the subband centre and the integration limits $\tilde{\nu}_1$ and $\tilde{\nu}_2$ refer to the wavenumbers where the absorption can be considered negligible. Following Amrein et al. [25], within each polyad block $N(\Gamma)$ (where $\Gamma = A'$ or A'', the symmetry species of the vibrational states) the observed relative band strengths $g_j^N(obs)$ are calculated from the experimental G_j^N employing the following expression:

$$g_j^N(obs) = \frac{G_j^N}{\sum_{N(\Gamma)} {}_k G_k^N} \quad . \tag{10}$$

These observed values can be compared with the corresponding relative intensities computed from the eigenvector matrix $\mathbf{Z}^N$. For each polyad labelled by an integer value of *N*, the chromophore state corresponds to the zero-order basis state having the largest value of v_1, the vibrational quantum number of the CH stretching mode; for the polyads with half integer value of *N* there are two of these chromophore states, one having $v_1 = N - 1/2$, $v_2 = 1$, $v_7 = 0$ the other with $v_1 = N - 1/2$, $v_2 = 0$, $v_7 = 1$. For the polyads having *N* = integer, one makes the assumption that only one state (i.e. the chromophore) carries zero-order intensity. The other bands of the polyad borrow their observed intensity entirely from anharmonic resonances with the chromophore. Under these hypotheses the relative intensity g_j^N of the transition from the ground state to the N_j vibrational level can be computed by considering the corresponding element of the eigenvector matrix $\mathbf{Z}^N$:

$$g_j^N = \left| Z_{1j}^N \right|^2 . \tag{11}$$

For the polyads having *N* = half integer, the two chromophore states are assumed to carry oscillator strength. In this case, the relative intensities are computed employing the following weighted average [26]:

$$g_j^N = \frac{\left|Z_{bj}^N\right|^2 + f\left|Z_{aj}^N\right|^2}{f+1} \quad (12)$$

where b and a are the indexes of the chromophore states having $v_1 = N - 1/2$, $v_2 = 1$, $v_7 = 0$ and $v_1 = N - 1/2$, $v_2 = 0$, $v_7 = 1$, respectively. The weighting factor f is given by the experimental intensity ratio of the first two components of the $N = 3/2$ polyad:

$$f = \frac{G_1^{3/2}}{G_2^{3/2}} \, . \quad (13)$$

5. Results and discussion

An overall survey of spectra concerning the CH chromophore transitions observed in the present work is presented in Figure 2. As it can be seen, all the most relevant absorptions above 4000 cm^{-1} are associated to various CH polyads, thus confirming the relevance of the CH chromophore in the NIR region of the spectra of bromodifluoromethane, being the contributions of hot bands negligible. The two fundamentals v_2 (A' symmetry) and v_7 (A'' symmetry) are shown in Figure 2(a). They are labelled as $1/2_2$ and $1/2_1$, respectively and form the lowest polyad. Moving to higher wavenumbers, in the spectral range 2500 – 3100 cm^{-1} one can assign the $N = 1$ polyad, illustrated in Figure 2(b). The strongest feature is assigned to the v_1 fundamental (A' symmetry) and it corresponds to the CH-stretching mode. It is located at 3020.9 cm^{-1} and labelled as 1_1. The other bands involved in this polyad, shown in the inset of Figure

2(b), are $2\nu_7$ (1_2) at 2676.1 cm^{-1}, $\nu_2 + \nu_7$ (1_3) and $2\nu_2$ (1_4) at 2628.8 and 2544.2 cm^{-1}, respectively, with an intensity which is almost three orders of magnitude lower than ν_1. The next two polyads, N = 3/2 and N = 2, reported in Figure 2(c), account for almost all the relevant absorptions falling in the range 4000 – 6000 cm^{-1}. Even if the conventional nomenclature in terms of combinations of different normal modes is not well suited when moving to higher wavenumbers, due to the relevant mixing among the vibrational states, we have tried a possible labelling of each absorption in the polyads in such manner. The $\nu_1 + \nu_7$ (4349.9 cm^{-1}) and $\nu_1 + \nu_2$ (4286.5 cm^{-1}) combination bands, indicated respectively as $3/2_1$ and $3/2_2$, are the first two components of the N = 3/2 polyad, while the most intense components of the N = 2 polyads, located at higher wavenumbers, are clearly visible. The CH polyads N = 5/2, N = 3 and N = 7/2 are shown in Figure 2(d). In the N = 3 polyad the most intense feature belongs to $3\nu_1$ (3_1) at 8712.2 cm^{-1}, while the weakest absorption assigned is $\nu_1 + 4\nu_2$ (3_9), reported in the inset of the same Figure. It has an observed relative band strength approximately three orders of magnitude lower than $3\nu_1$.

A total of 26 transitions belonging to different CH polyads (up to N =7/2) were assigned in the present work. After having set up all the matrix elements of the effective vibrational Hamiltonian for each of the considered polyads, the spectroscopic parameters collected in Table 1 have been derived by least-square fitting the resulting eigenvalues with all the corresponding wavenumbers of the experimentally observed band centres. The column labelled Fit 1 lists the results computed letting all the twelve parameters of the effective Hamiltonian free to vary. The reported values clearly show the Fermi coupling between the CH-stretching and the CH-bending modes, being the corresponding resonance parameters k'_{122} and k'_{177} equal to 95 and 87.6 cm^{-1},

respectively. In addition, also the value for the Darling-Dennison resonance term k'_{2277} = 10.4 cm^{-1} suggests some effects of this coupling on the various overtones and combination bands within the polyads. The x'_{11} anharmonicity constant has a value (-61.8 cm^{-1}) very similar to those found for analogous halogenated methanes such as $CHClF_2$ [25] and $CHCl_2F$ [27] (x'_{11} = -63.8 cm^{-1} and -63.1 cm^{-1}, respectively). Without taking into account the Fermi resonances related to k'_{122} and k'_{177}, the values of x'_{11} and $\tilde{\nu}'_1$ obtained from the fit of ν_1, $2\nu_1$ and $3\nu_1$ are -57.3 and 3075.7 cm^{-1}, respectively. The small differences between these results and those obtained by introducing the off diagonal coupling terms can be rationalized by considering that in each polyad (with $N = n$) the energy separation between the zero-order states $n\nu_1$ and $(n\text{-}1)\nu_1+2\nu_2$ or $(n\text{-}1)\nu_1+2\nu_7$ is generally greater than the values of the corresponding off diagonal matrix elements. However, as before without considering explicitly the coupling terms, the comparison of the value of x'_{11} determined from $2\nu_1$ and ν_1 (x'_{11} = -61.05 cm^{-1}) with that obtained from $3\nu_1$ and ν_1 (x'_{11} = -58.4 cm^{-1}) suggests a trend understandable on the basis of an increasing ratio of the off diagonal matrix elements to the corresponding zero-order state energy differences.

The other diagonal anharmonicity constant values, x'_{22} = -6.8 cm^{-1} and x'_{77} = -7.6 cm^{-1}, are close to that expected for an isolated CH-chromophore, while the mixed anharmonicity constants x'_{12} and x'_{17} (-25.8 and -25.7 cm^{-1}, respectively) are in the range of the values obtained for other halogenated methane derivatives [24 – 28]. A further evidence for the need of a global model is given by the comparison of the x'_{ij} constant values with those obtained by the differences $(n\nu_i+\nu_j) - n\nu_j - \nu_j$ without taking

into account any interaction. For example, the anharmonicity constant $x_{17}^{'}$ obtained for n = 1 is -16.5 cm^{-1}, while for n = 3 it becomes -9.80 cm^{-1}.

In general, all the parameters obtained are well determined, the only one whose uncertainty is within its magnitude is the anharmonicity constant $x_{27}^{'}$, whose value is anyway close to zero. Therefore, we tried to fix this constant in the fitting procedure thus obtaining the parameters reported in the column Fit 2 of Table 1. There is not a significant difference between the values of Fit 1 and Fit 2, only a slight increase in the root-mean-square deviation, here calculated on the base of the sum of the squares of the deviations between the observed and the computed values, divided by the number of data, occurs (from 1.26 cm^{-1} for Fit 1 to 1.33 cm^{-1} for Fit 2). Table 2 reports the experimental and the predicted vibrational wavenumbers and relative intensities for all the observed bands. The agreement between the experimental data and those computed by the effective Hamiltonian is very good. For the band centres, the fit with 12 degrees of freedom (mean absolute error = 0.896 cm^{-1}, mean signed error = -0.0752 cm^{-1}) and that with 11 degrees of freedom (mean absolute error = 0.895 cm^{-1}, mean signed error = -0.0425 cm^{-1}) perform equally well in predicting the experimental transitions. The predicted relative intensities were computed, as previously outlined, under the hypothesis that only the chromophore state carries oscillator strength; anyway, the model appears able to reproduce, at least semi-quantitatively, the observed values. The discrepancies can be ascribed not only to additional local resonances not explicitly considered by the Hamiltonian employed in the present study, but also to the presence, in some integration ranges, of other bands. The magnitude of the deviations is comparable to that reported by other authors [24, 26]. No significant differences between the values computed employing the fit with 12 degrees of freedom and those

obtained from the fit with 11 degrees of freedom have been found, therefore in Table 2 we reports the value derived from the former.

The model of the Hamiltonian here employed considers only intrapolyad resonances, thus not taking into account the possibility of interpolyad coupling among different blocks belonging to the same symmetry species. Nevertheless, the energy separation among consecutive polyads is so great compared to the coupling matrix elements to make it possible to neglect the corresponding perturbation effects.

The results obtained employing the above described least square analysis can be compared with those obtained from an *ab initio* study of the CH absorptions. Recalling that the CH chromophore comprises the ν_1, ν_2 and ν_7 vibrational modes and that these normal modes are expected to be in resonance, the diagonal matrix elements of the polyads are the wavenumbers obtained from:

$$\langle \mathrm{v} \mid H \mid \mathrm{v} \rangle = \sum_r \omega_r (\mathrm{v}_r + \frac{1}{2}) + \sum_{r \le s} x_{rs} (\mathrm{v}_r + \frac{1}{2})(\mathrm{v}_s + \frac{1}{2}) \qquad (14)$$

where the anharmonicity constants x_{rs} calculated from the *ab initio* force field must be replaced with x_{rs}^* constants, which exclude those second-order perturbation theory contributions that are included explicitly in the Fermi resonance model. The out diagonal terms are the Fermi resonances, through the φ_{rss} cubic force constants (r = 1, s = 2 or 7),

$$\langle \mathrm{v}_r, \mathrm{v}_s \mid H_F \mid \mathrm{v}_r - 1, \mathrm{v}_s + 2 \rangle = \frac{\varphi_{rss}}{4} \left[\frac{\mathrm{v}_r (\mathrm{v}_s + 1)(\mathrm{v}_s + 2)}{2} \right]^{1/2} \qquad (15)$$

and Darling-Dennison resonance interactions between the overtone levels of CH in-plane and out-of-plane deformations

$$\left\langle \mathrm{v}_r + 2, \mathrm{v}_s \mid H_{D-D} \mid \mathrm{v}_r, \mathrm{v}_s + 2 \right\rangle = \frac{K_{rrss}}{4}\left[(\mathrm{v}_r + 1)(\mathrm{v}_r + 2)(\mathrm{v}_s + 1)(\mathrm{v}_s + 2)\right]^{1/2} \qquad (16)$$

where K_{rrss} (r = 2, s = 7) is the Darling-Dennison coupling constant which is computed from cubic and quartic force constants, rotational constants, Coriolis terms and harmonic wavenumbers.

Removing the offending terms, $\varphi_{rss}^2 / (2\omega_s - \omega_r)$, from second order expressions, the anharmonicity constants result x_{12}^* = -58.106, x_{17}^* = -60.610, x_{22}^* = 2.906, x_{77}^* = 2.451 (in units of cm^{-1}). The unperturbed values for the bands of A' symmetry involved in the N = 1 polyad thus become 2974 cm^{-1} (ν_1), 2542 cm^{-1} ($2\nu_2$) and 2656 cm^{-1} ($2\nu_7$). The Hamiltonian matrix after diagonalization gives 3026 cm^{-1} (ν_1), 2501 cm^{-1} ($2\nu_2$) and 2645 cm^{-1} ($2\nu_7$). Whereas the ν_1 fundamental value is close to that obtained without considering the resonance and to the experimental one, the $2\nu_2$ and $2\nu_7$ computed wavenumbers are in disagreement with the experimental data. In addition, considering the higher overtones and combination bands,

$$(n\nu_1 + m\nu_2 + l\nu_7) = n(\nu_1) + m(\nu_2) + l(\nu_7) + n(n-1)x_{11} + m(m-1)x_{22}^* +$$

$$+ l(l-1)x_{77}^* + (n \cdot m)x_{12}^* + (n \cdot l)x_{17}^* + (m \cdot l)x_{27}^* \qquad (17)$$

the Hamiltonian matrix after diagonalization gives wavenumbers having errors as large as 300 cm^{-1} when compared to the observed ones. One of the reason is certainly due to the large values of the *ab initio* cubic force constants φ_{122} = -447.3 cm^{-1} and φ_{177} = -409.0 cm^{-1} that appear too large. The issue of unusually large values of cubic force constants has been already pointed out in other investigations. Examples are given by the studies carried out by Law and co-workers [29, 30], the calculation of spectroscopic parameters of methanol performed by Hänninen and Halonen [31] as well as the VPT approach of Matthews et al. to the stretching overtone levels of water vapour [32]. Although Law and Duncan demonstrated that a better agreement between *ab initio* cubic force constants and empirical Fermi parameters may be obtained by including corrections from second order perturbation theory, they also emphasized that these terms do not provide a complete description of the Fermi resonance. Therefore we have investigated the possibility of higher-order effects in this model including the dependence of the interacting levels from the vibrational quantum numbers into the Fermi coupling constants. Although for the polyad with N = 1 a slight improvement could be observed, on average no significant improvements have been obtained from this approach. If the presence of strong Fermi resonances could be easily recognized from the unusual values of the anharmonicity constants, it is very difficult, if not impossible, to find a simple criterion for the recognition of weak Fermi interactions. A working expression for the estimate of higher order effects has been proposed by Martin et al. [33] who, for type-1 Fermi resonance (i.e. ν_1, $2\nu_1$), derived the quantity $\varphi_{rss}^4 / 256(2\omega_s - \omega_r)^3$. In our case the effects are 1.048 and 1.605 for $\nu_1/2\nu_2$ and $\nu_1/2\nu_7$, respectively, thus suggesting that the higher order effects affecting ν_1 are weak. In

addition, the small deviations of x_{11} in a so-called Birge-Sponer plot [34] suggest very weak resonances for this vibrational mode. This is in agreement with the experimental observation that neglecting Fermi resonances from the least squares analysis of the assigned absorptions has little effect on the value of $x_{11}^{'}$ anharmonicity constant.

On the basis of these observations, we have simplified the model by excluding Fermi resonances and taking into account all Darling-Dennison resonances between overtones and combinations of the CH bending modes within each polyad up to $N = 7/2$. The same approach has also been adopted by Hänninen and Halonen in their study on methanol [31] who have not been able "to obtain any improvement" by including higher order effects and hence, in the final calculation they excluded Fermi interaction between the OH stretch and CH bend. The calculated wavenumbers corresponding to the observed ones are reported under the *ab initio* column of Table 2. There is a general agreement between the observed and calculated values, even if, on average, the computed values fall at higher wavenumbers than the experimental ones (mean signed error = -7.7 cm^{-1}). Concerning the CH chromophore states up to $N = 5/2$ the differences between the observed wavenumbers and those computed *ab initio* are generally within 10 cm^{-1}; going to higher polyads these differences tend to increase but they still remain lower than 20 cm^{-1}.

Conclusions

The vibrational analysis of the gas phase infrared spectra of bromodifluoromethane, $CHBrF_2$, performed by means of an effective Hamiltonian confirms the validity of the CH chromophore framework also for this molecule. The

good agreement between the experimental and the predicted wavenumbers demonstrates the usefulness of this model to quantitatively describe the most relevant resonances affecting the absorptions in the overtone region up to 10100 cm^{-1}. The approach here followed is of central importance to understand the role of Fermi and Darling-Dennison coupling terms between the CH-stretching and bending modes as well as in modelling the features of the spectra of $CHBrF_2$ in the near infrared region.

Employing the VPT2 spectroscopic parameters, the *ab initio* resonant model used to describe the CH chromophore polyads, which excludes Fermi resonances due to the high values of the computed cubic force constants φ_{122} and φ_{177}, and considers only Darling-Dennison resonances between the overtones of ν_2 and ν_7, leads to an overall satisfactory agreement with the experimental data and also it could be useful to follow the correct assignment of the bands here considered.

In conclusion, this work provides the first description of the different CH chromophore polyads which accounts for almost all the most relevant absorptions of $CHBrF_2$ up to the near infrared region of the spectra. The information here reported is useful for successive studies which could better determine the resonances here analyzed.

Acknowledgments

The High Performance Systems Division of the CINECA Supercomputer Centre Interuniversity Consortium is gratefully acknowledged for support in the utilization of computer resources. One of the authors (N. T.) gratefully acknowledges Universita' Ca' Foscari Venezia for his post-doc grant.

References

[1] M. Quack, Ann. Rev. Phys. Chem. **41**, 839 (1990).

[2] M. Gruebele, P. G. Wolynes, Acc. Chem. Res. **37**, 261 (2004).

[3] F.F. Crim, J. Phys. Chem. **100**, 12725 (1996).

[4] D.W. Lupo, M. Quack, Chem. Rev. **87**, 181 (1987).

[5] M. Quack, Infrared Phys. Technol. **36**, 365 (1995).

[6] A. C. Brown, C. E. Canosa-Mas, A. D. Parr, K. Rothwell, R. P. Wayne, Nature **347**, 541 (1990).

[7] R. Talukdar, A. Mellouki, T. Gierczak, J. B. Burkholder, S. A. McKeen, A. R. Ravishankara, Science **252**, 693 (1991).

[8] V. L. Orkin, V. G. Khamaganov, J. Atmos. Chem. **16**, 169 (1993).

[9] S. Kuribayashi, T. Tomimasu, S. Kawanishi, S. Arai, Appl. Phys. B **65**, 393 (1997).

[10] S. Arai, K. Ikawa, Y. Matsumoto, Y. Iizuka, K. Sugita, S. K. Sarkar, S. Kuribayashi, Nucl. Instrum. Meth. Phys. Res. B **144**, 193 (1998).

[11] A. Pietropolli Charmet, P. Stoppa, N. Tasinato, A. Baldan, S. Giorgianni, A. Gambi, J. Chem. Phys. **133**, 044310 (2010).

[12] G. Cazzoli, L. Cludi, C. Puzzarini, P. Stoppa, A. Pietropolli Charmet, N. Tasinato, A. Baldacci, A. Baldan, S. Giorgianni, R. W. Larsen, S. Stopkowicz, J. Gauss, J. Phys. Chem. A **115**, 453 (2011).

[13] H. –R. Dübal, M. Quack, Chem. Phys. Lett. **72**, 342 (1980).

[14] Mills, I. M. *Molecular Spectroscopy: Modern Research*, edited by Narahari, Rao K.; Mathews, C. W., Academic Press, New York, 1972; Vol. 1, pp 115–140.

[15] V. L. Orkin, A. G. Guschin, I. K. Larin, R. E. Huie, M. J. Kurylo, J. Photochem. Photobiol., A **157**, 211 (2003).

[16] P. Stoppa, A. Pietropolli Charmet, N. Tasinato, S. Giorgianni, A. Gambi, J. Phys. Chem. A **113**, 1497 (2009).

[17] A. Pietropolli Charmet, N. Tasinato, P. Stoppa, A. Baldacci, S. Giorgianni, Mol. Phys. **106**, 1171 (2008).

[18] G. D. Purvis III, R. J. Bartlett, J. Chem. Phys. **76**, 1910 (1982).

[19] K. Raghavachari, G. W. Trucks, J. A. Pople, M. Head-Gordon, Chem. Phys. Lett. **157**, 479 (1989).

[20] T. H. Dunning Jr., J. Chem. Phys **90**, 1007 (1989); D. E. Woon, T. H. Dunning Jr., J. Chem. Phys. **98**, 1358 (1993); R. A. Kendall, T. H. Dunning Jr., R. J. Harrison, J. Chem. Phys. **96**, 6796 (1992).

[21] X. –G. Wang, E. L. Sibert III, J. M. L. Martin, J. Chem. Phys. **112**, 1353 (2000).

[22] W. Schneider, W. Thiel, Chem. Phys. Lett. **157**, 367 (1989).

[23] D. C. McKean, N. C. Craig, M. M.Law, J. Phys. Chem. A **112**, 6760 (2008); W. D. Allen, A. G. Császár, D. A. Horner, J. Am. Chem. Soc. **114**, 6834 (1992).

[24] V. Horká, M. Quack, M. Willeke, Mol. Phys. **106**, 1303 (2008).

[25] A. Amrein, H. –R. Dübal, M. Quack, Mol. Phys. **56**, 727 (1985).

[26] A. Beil, D. Luckhaus, M. Quack, Ber. Bunsenges. Phys. Chem. **100**, 1853 (1996).

[27] H.-R. Dübal, M. Quack, Mol. Phys. **53**, 257 (1984).

[28] D. Luckhaus, M. Quack, Chem. Phys. Lett. **190**, 581 (1992).

[29] M. M. Law, J. L. Duncan, Chem. Phys. Lett. **212**, 172 (1993).

[30] D. C. McKean, N. C. Craig, M. M. Law, J. Phys. Chem. A **112**, 10006 (2008).

[31] V. Hänninen, L. Halonen, Mol. Phys. **101**, 2907 (2003).

[32] D. A. Matthews, J. Vázquez, J. F. Stanton, Mol. Phys. **105**, 2659 (2007).

[33] J. M. L. Martin, T. J. Lee, P. R. Taylor, J-P. François, J. Chem. Phys. **103**, 2589 (1995).

[34] R. T. Birge, H. Sponer, Phys. Rev. **28**, 259 (1926).

Table 1. Spectroscopic parameters (cm^{-1}) of $CHBrF_2$ obtained from least square fitting to the model Hamiltonian [a]

Parameter	Fit 1 [b]	Fit 2 [c]
$\tilde{\nu}_1'$	3072.2(13)	3072.4(14)
$\tilde{\nu}_2'$	1289.5(15)	1288.9(15)
$\tilde{\nu}_7'$	1355.1(18)	1354.6(17)
x_{11}'	-61.8(11)	-61.9(11)
x_{12}'	-25.8(25)	-26.2(26)
x_{17}'	-25.7(26)	-26.5(27)
x_{22}'	-6.8(9)	-6.6(9)
x_{27}'	-1.0(8)	0 [d]
x_{77}'	-7.6(1.1)	-7.5(12)
k_{122}'	95(11)	95(12)
k_{177}'	87.6(77)	89.7(78)
k_{2277}'	10.4(16)	10.9(16)
N. data	26	26
RMS	1.26	1.33
σ_{fit}	1.71	1.76

[a] Figures in parentheses correspond to one standard deviation.
[b] Least square fitting with 12 degrees of freedom.
[c] Least square fitting with 11 degrees of freedom.
[d] Constrained.

Table 2 (1 of 2). Experimental and predicted vibrational wavenumbers and relative intensities of $CHBrF_2$ within a given polyad

Band	Symmetry	N_j	$\tilde{\nu}_0$ [cm^{-1}] Observed [a]	Fit 1 [b]	Fit 2 [c]	*Ab initio* [d]	g_{rel}^{obs} [e]	g_{rel}^{fit} [f]
ν_2	A'	$1/2_2$	1282.1(3)	1282.7	1282.3	1282.5	0.9027	0.7359
ν_7	A''	$1/2_1$	1346.5(3)	1347.4	1347.1	1340.8	0.0973	0.2641
$2\nu_2$	A'	1_4	2544.2(3)	2545.1	2544.8	2544.1	0.0266	0.0123
$\nu_2 + \nu_7$	A''	1_3	2628.8(5)	2629.1	2629.5	2624.2	0.0150	0.0000
$2\nu_7$	A'	1_2	2676.1(3)	2675.9	2675.5	2664.1	0.0370	0.0124
ν_1	A'	1_1	3020.9(3)	3020.5	3020.9	3023.2	0.9355	0.9750
$3\nu_2$	A'	$3/2_3$	3789.6(3)	3789.0	3789.0	3794.3	0.0102	0.0240
$\nu_1 + \nu_2$	A'	$3/2_2$	4286.5(3)	4286.3	4286.1	4294.8	0.7387	0.7057
$\nu_1 + \nu_7$	A''	$3/2_1$	4349.9(5)	4352.4	4352.2	4354.6	0.2613	0.2509
$\nu_1 + 2\nu_2$	A'	2_4	5528.7(3)	5528.9	5528.5	5545.4	0.1063	0.0356
$\nu_1 + 2\nu_7$	A'	2_2	5661.5(1.0)	5661.7	5661.0	5668.4	0.0696	0.0397
$2\nu_1$	A'	2_1	5919.7(3)	5922.4	5923.0	5922.4	0.8242	0.9234
$\nu_1 + 3\nu_2$	A'	$5/2_6$	6750.9(3)	6751.3	6751.1	6777.6	0.0517	0.0644
$\nu_1 + 2\nu_2 + \nu_7$	A''	$5/2_5$	6851.2(1.0)	6851.2	6851.6	6868.5	0.0330	0.0163
$\nu_1 + \nu_2 + 2\nu_7$	A'	$5/2_4$	6930.2(3)	6928.2	6929.2	6945.6	0.0269	0.0205
$2\nu_1 + \nu_2$	A'	$5/2_2$	7176.4(3)	7174.3	7174.1	7183.0	0.5525	0.6491
$2\nu_1 + \nu_7$	A''	$5/2_1$	7246.5(2.0)	7243.7	7243.4	7255.3	0.3359	0.2256
$\nu_1 + 4\nu_2$	A'	3_9	7954.3(5)	7954.0	7954.3	7991.1	0.0038	0.0024
$\nu_1 + 2\nu_2 + 2\nu_7$	A'	3_7	8146.6(3)	8146.5	8146.6	8167.7	0.0090	0.0046
$2\nu_1 + 2\nu_2$	A'	3_4	8396.4(3)	8397.2	8396.7	8422.8	0.1170	0.0845

Table 1. (Continued 2 of 2)

Band	Symmetry	N_j	$\tilde{\nu}_0$ [cm^{-1}]				g_{rel}^{obs} [e]	g_{rel}^{fit} [f]
			Observed [a]	Fit 1 [b]	Fit 2 [c]	*Ab initio* [d]		
$2\nu_1 + \nu_2 + \nu_7$	A''	3_3	8494.0(3)	8493.5	8493.7	8505.8	0.0107	0.0000
$2\nu_1 + 2\nu_7$	A'	3_2	8533.5(2.0)	8532.9	8532.0	8548.7	0.1301	0.1106
$3\nu_1$	A'	3_1	8712.2(3)	8711.7	8712.2	8697.6	0.7294	0.7966
$2\nu_1 + \nu_2 + 2\nu_7$	A'	$7/2_4$	9783.9(3)	9786.2	9786.9	9814.9	0.2399	0.0534
$3\nu_1 + \nu_2$	A'	$7/2_2$	9953.9(3)	9953.7	9953.4	9947.3	0.5046	0.5372
$3\nu_1 + \nu_7$	A''	$7/2_1$	10029.3(1.0)	10030.0	10029.9	10010.1	0.2556	0.1767

[a] Figures in parentheses represent experimental errors.
[b] Predicted from parameters obtained by least square fitting with 12 degrees of freedom.
[c] Predicted from parameters obtained by least square fitting with 11 degrees of freedom.
[d] Predicted from *ab initio* hybrid force field: geometry and quadratic force constants at CCSD(T)/cc-pVTZ (for H, C, Br atoms) and CCSD(T)/aug-cc-pVTZ (F atoms); cubic and quartic force constants at CCSD(T)/cc-pVTZ.
[e] Observed relative intensities within a given polyad block.
[f] Relative intensities within a given polyad block predicted by least square fitting with 12 degrees of freedom.

Figure captions

Figure 1. Approximate description of $CHBrF_2$ normal modes of vibration involving the C-H chromophore: (a) ν_1, stretching; (b) ν_2, in-plane bending; (c) ν_7, out-of-plane bending. Vectors represent atomic displacements during vibrational motion.

Figure 2. Vibrational spectra of $CHBrF_2$ in the regions of the ν_1, ν_2 and ν_7 fundamentals and their overtones.

(a) N = 1/2 polyad in the 1000 – 1400 cm^{-1} spectral region (experimental conditions: pressure = 10.0 mbar; optical path = 13.4 cm; resolution = 0.5 cm^{-1}; temperature = 298 K).

(b) N = 1 polyad in the 2000 – 3200 cm^{-1} spectral region (experimental conditions: pressure = 30.9 mbar; optical path = 13.4 cm; resolution = 0.5 cm^{-1}; temperature = 298 K); the inset shows a magnified view of overtones and combination bands belonging to this polyad.

(c) N = 3/2 and N = 2 polyads within the 4000 – 6500 cm^{-1} spectral region (experimental conditions: pressure = 33 mbar; optical path = 10.5 m; resolution = 0.5 cm^{-1}; temperature = 298 K).

(d) N = 5/2, N = 3 and N = 7/2 polyads in the 6500 – 10000 cm^{-1} spectral region (experimental conditions: pressure = 33 mbar; optical path = 77.5 m; resolution = 0.5 cm^{-1}; temperature = 298 K). The inset shows a magnified view of the 7900 – 8200 cm^{-1} interval where $N = 3_9$ ($\nu_1 + \nu_4$) and $N = 3_7$ (ν_1

+ $2\nu_2 + 2\nu_7$) combinations have been observed.

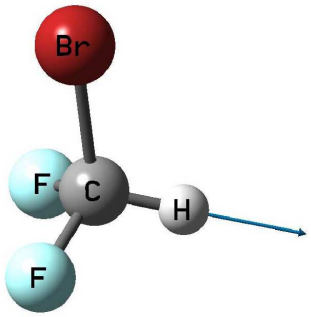

Figure 1(a)

210x297mm (600 x 600 DPI)

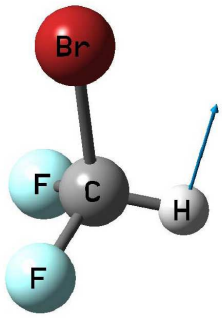

Figure 1(b)

210x297mm (600 x 600 DPI)

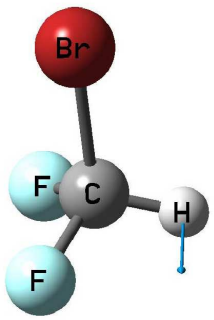

Figure 1(c)

210x297mm (600 x 600 DPI)

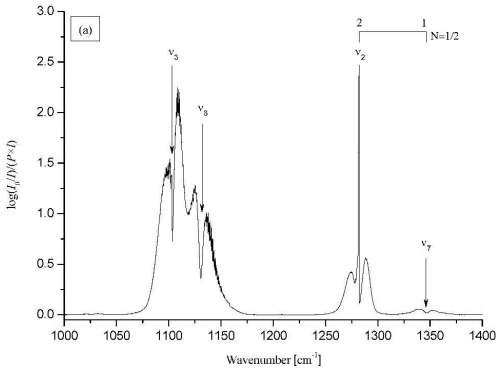

Figure 2(a)

210x297mm (600 x 600 DPI)

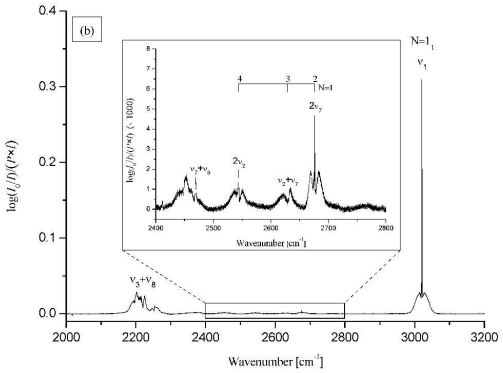

Figure 2(b)

210x297mm (600 x 600 DPI)

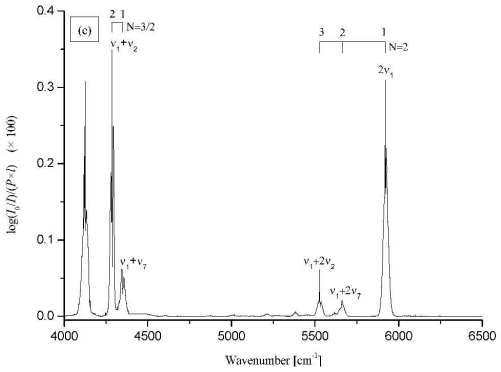

Figure 2(c)

210x297mm (600 x 600 DPI)

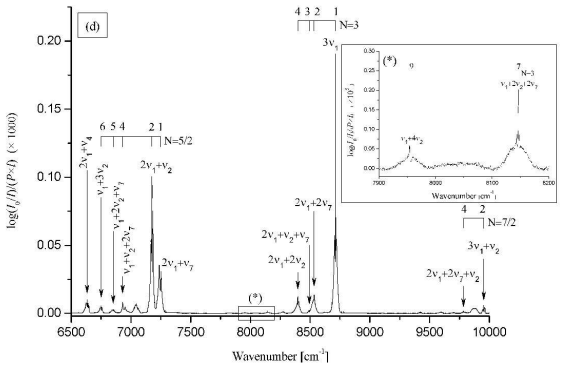

Figure 2(d)

210x297mm (600 x 600 DPI)